International Journal of Civil Engineering

Structure

Earthquake

Input waves for seismic design of power substation equipment for near and far Iranian earthquake records

M. Bastami[1,]*, M. Hajihasani[2]

Received: June 2012, Revised: August 2013, Accepted: October 2013

Abstract

Dynamic analysis of the seismic performance of power substation equipment is time-consuming, expensive and uses responses that are sensitive to ground motion. This research proposes a method to derive input waves for dynamic analysis in place of original records from seismic events in Iran. In this study, a power transformer, current transformer, circuit breaker and disconnect switch are analyzed using fifty records from the far-field and near-field earthquake ground motions. Statistical analysis is done on the maximum acceleration and displacement responses to obtain their pushover curves. Sinusoidal waves were created using the fundamental frequencies of the equipments and PGA of 0.1g through 0.5 g as the amplitude. Compared with the original records, the results show that the proposed input waves provide a reasonable fit for an extensive range of near-field and far-field ground motion results.

Keywords: *Input wave, Seismic analysis, Power substation, Power transformer, Current transformer, Circuit breaker, Disconnect switch.*

1. Introduction

Electrical networks are important lifelines after a natural disaster such as earthquakes. They are essential for lighting, heating, and ventilation as well as the continued operation of telecommunications, all types of transportation and traffic control, and commercial and industrial activities. Power substations are the most vulnerable elements of a power supply system all over the world [1]. In this research, seismic behavior and seismic evaluation procedures are studied for key equipment operating in a power substation with an emphasis on power transformers, current transformers, live-tank circuit breakers, and disconnect switches. This research provides input waves for dynamic analysis of electrical substation equipment in Iran. For this purpose, fifty major earthquake ground motion records with magnitudes greater than six in far and near fields from the Iran Strong Motion Network (ISMN) are used [2].

Ground motion of the near field has a more limited frequency domain than that of the far field, and its energy is transmitted in a limited frequency domain. Major elastic seismic energy is transmitted with an intense pulse over a long period, usually at the beginning of the record.

Furthermore, a near-field record contains pulse-like excitation instead of having a time history with broadband frequency content.

This means that the Fourier spectral domain is the maximum value in a very small range or specific period instead of an extensive range or period. Another criterion for a near-field motion is that the distance from the earthquake epicenter is less than a specific distance. A number of researchers consider this distance to be 20 km, while others suggest 15 km [3].

Near-field ground motions typically have higher PGV to PGA ratios than far field motions. Moreover, they have a pulse-like motion, especially at the beginning of the record and produce seismic energy in a short period. Longitudinal acceleration, velocity and displacement generate an impact force on structures; and the ratio of vertical peak acceleration to horizontal peak acceleration in the records is greater for near field than for far field [3]. Figures 1-3 show acceleration, velocity and displacement histories of the 1990 Roodbar-Manjil (Abbar station) and 1978 Tabas earthquakes (far-field records), and the 2003 Bam earthquake (near-field record), respectively.

In this study, equipment modeled using the 3-D finite-element method (FEM) after performance modal analyses to obtain their natural frequencies are subjected to time-history analysis using a records collection. The maximum displacement and acceleration at critical points are recorded for far field and near field ground motions. Then, using a technique similar to the one proposed by the Japan Electric Association Guidelines, JEAG-5003-1999, for power substation equipment, sinusoidal waves were created using the fundamental frequencies and PGA of 0.1

* *Corresponding author: m.bastami@iiees.ac.ir*
1 International Institute of Earthquake Engineering and Seismology, N. Dibaji St., No. 21, Tehran, Iran
2 Imam Khomeini International University, Qazvin, Iran

g, 0.15 g, 0.2 g, 0.25 g, 0.3 g, 0.35 g, 0.4 g, 0.45 g and 0.5 g as the amplitude of the sine waves [4]. The Japanese Guideline technique was developed for a one degree of freedom system composed of a lumped mass and spring for the complex substation equipment. In this study, the equipment is modeled using 3-D FEM in order to validate the technique for Iran. Finally, the results of analysis under 50 actual records and the sine waves are compared for the far field and near field to propose the final appropriate sinusoidal waves for the equipment. This final step was not taken into account in the Japan Guidelines.

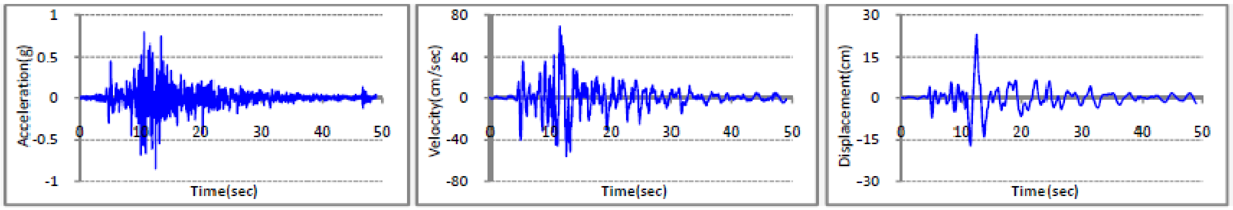

Fig. 1 Acceleration, velocity and displacement histories of 1978 Tabas earthquake

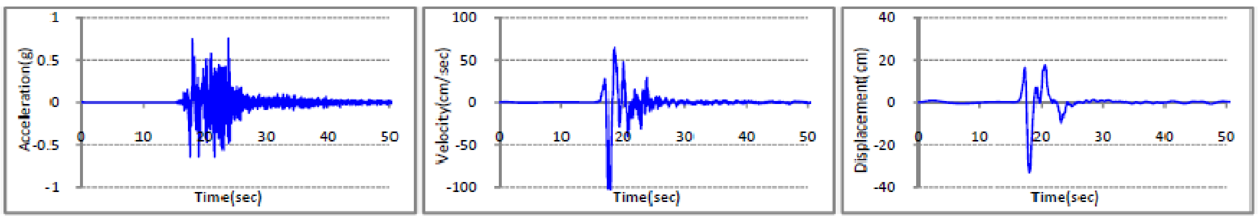

Fig. 2 Acceleration, velocity and displacement histories of 2003 Bam earthquake

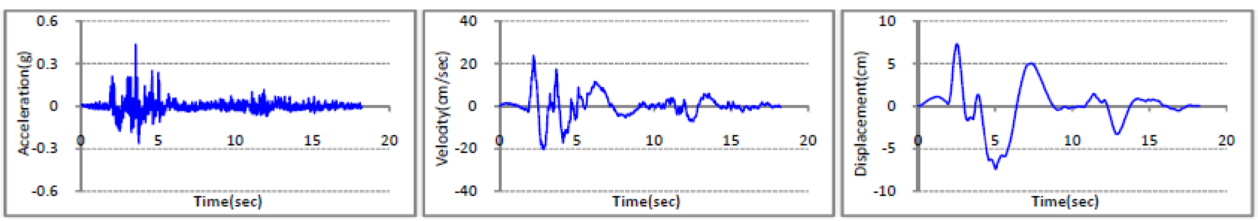

Fig. 3 Acceleration, velocity and displacement histories of 1990 Roodbar-Manjil earthquake (Abbar station)

2. Literature Review

Recent experimental and theoretical research has evaluated the seismic performance of substation components with an emphasis on transformers and porcelain bushings. Bellorini et al. did experimental tests and finite element analysis of a 230 kV transformer to determine the dynamic properties of the transformer and evaluate the ground motion amplification at the bushing flange center of gravity [5]. Gilani et al. conducted shaking tests on the seismic performance of 230 and 550 kV porcelain transformer-bushings [6-7]. Kiureghian et al. studied the interaction of substation equipment [8]. Villaverde et al. quantified ground motion amplification occurring at the base of bushings mounted on electric substation transformers [9]. It was determined that the amplification factors for the 500 kV bushings were within a factor of 2.0, as specified by Standard IEEE 693. However, the 230 kV bushings exceeded the IEEE 693 amplification by a factor of 2.0 (IEEE, 1997) [10].

Matt and Filiatrault researched the seismic response of five power transformers [11]. Time history analyses were performed to determine the dynamic response and amplification at the base of the transformer bushing. The highest amplifications occurred when the two natural frequencies were close.

Su et al. developed a method to calculate accelerograms to match a design target spectrum for appropriate earthquake magnitude, distance, and site conditions [12]. They found that the shape of the response spectra exhibited strong magnitude and site dependency and weak distance dependency. Thus, the normalized spectra from a large earthquake recorded on a soft soil site are likely to exceed IEEE 693-1997 over long periods. Takhirov et al. developed a set of earthquake ground strong motion time histories suitable for seismic qualification testing of electrical substation equipment in accordance with IEEE 693-1997 [13]. Some 35 three-component historic records from 18 earthquakes were analyzed and cross-compared based on several parameters, and the best candidate for input strong motion was selected and modified. The resulting strong motion time history preserved the non-stationary behavior of the real earthquake record while its response spectra enveloped the IEEE target response spectra in a broad range of natural frequencies, as required by the standard.

Saadeghvaziri et al. studied the advantages and considerations for the application of base isolation [14]. They found that base isolation can be highly effective in mitigating adverse interaction between transformers and bushings and have beneficial effects on the long-term longevity of transformers and on foundation performance. They developed a simplified model of the transformer bushing using a case study (433.3-MVA transformer in a high-voltage substation). Moreover, larger displacement was demonstrated and accommodated, thus, for this transformer, uplift was not an issue.

Koller et al. measured the frequencies of the fundamental rocking motions for five typical transformers to more comprehensively estimate the ground accelerations necessary to provoke partial uplift of power transformers [15]. The results showed that all transformers had natural rocking frequencies within the plateau range of common seismic design spectra. The conclusion was that power transformers should be anchored against uplift, even in areas of moderate seismicity.

Bastami [16] did a study to obtain fragility curves of a set of substation components in Power Supply Network of Tehran. He applied sinusoidal input waves recommended by the Japan Electric Association Guidelines, JEAG-5003-1999, for power substation equipments based on recorded ground motions of past earthquakes in Japan [4]. He proved feasibility of the method compared with results from the 1995 Kobe and the 2003 Bam ground motion records.

Japan Electric Association developed a guideline for seismic design of power-substation equipments, known as JEAG-5003. First version of the guideline was published in 1985 and it was revised in 1999 after the 1995 Kobe earthquake. The guideline proposes input waves to seismic design of the equipments. The input waves are recommended based on 615 recorded ground motions of past earthquakes in Japan. The proposed input waves are verified, by using amplification factors for one, two, and three waves by fundamental frequency with PGA of 0.5g (for power transformer) and 0.3g (for other equipments) for a single-freedom degree structure in comparison with the actual recorded ground motions of past earthquakes [4].

3. Modeling the Equipment

In previous earthquakes, i.e. Izmit Turkey-1999, Bam Iran-2003, Niigata Japan-2004, 2006 Western Iran, Niigata Chuetsu Japan-2007 Earthquakes, there are some damages to other parts of the transformer, and damages did not limit to the bushings [16]. As a result of the above experiences, we should consider all parts of the transformer.

The finite-element method provides a suitable platform to perform a reasonable evaluation of equipment response characteristics. Essential equipment for a power substation is the power transformer, current transformer, live-tank circuit breaker and disconnect switch, which are modeled in this study using 3-D FEM.

The transformer tank, reservoirs, steel pockets, porcelain and plates are modeled using shell elements. The mass of the oil in the transformer and reservoir are added to the mass of the transformer tank and reservoir. Braces, aluminum conductors, and stiffeners are modeled using beam elements. The core and coil inside the transformer are modeled as mass elements. The radiators are modeled using 3-D solid elements. The gaskets are continuous elements modeled by dividing the area between the 16 oriented elements. Tables 1 and 2 show the structural and geometric specifications of the equipment. The mechanical properties of the porcelain are based on results of a study at the International Institute of Earthquake Engineering and Seismology (IIEES) (Khalvati et al., 2011) [17]. Figure 4 shows four pieces of 230 kV equipment in a substation in Tehran modeled using the proper structural elements. Figure 5 shows all components of the finite-element modeling of the equipment.

Table 1 Structural and geometric specifications of 230 kv Power transformer

Specifications	Power transformer
Dimensions of main tank (m)	2.55*7.7*3.9
Total height of bushing (m)	4.24
Height of porcelain part (m)	3.6
Thickness of top plate of main tank (mm)	20
Dimension of stiffener of main tank (cm)	Plate 0.2*.02
Modulus of elasticity of aluminum core (MPa)	71000
Modulus of elasticity of porcelain (MPa)	99800
Modulus of elasticity of gasket (MPa)	48
Diameter of porcelain at bottom (cm)	30
Thickness of porcelain (cm)	3
Diameter of aluminum core (cm)	3.05
Type of support	Fixed
Number and size of volts in each support (mm)	4*M20

Table 2 Structural and geometric specifications of 230 kv current transformer, disconnect switch and circuit breaker

Specifications	Current transformer	Disconnect switch	Circuit breaker
Dimensions of main structure (m)	0.62*0.62	9.4*2.7	4.75*1.125
Height of main structure (m)	1.7	2.79	1.85
Total height of bushing (m)	3.65	2.45	4.02
Height of total system from top of foundation (m)	6.2	5.24	5.87
Section of brace elements (mm)	L50*50*6	L45*45*4	L45*45*4
Section of column elements (mm)	L65*65*8	L100*100*10	L70*70*8
Modulus of elasticity of steel parts (MPa)	206,000	206,000	206,000
Modulus of elasticity of porcelain (MPa)	99,800	99,800	99,800
Diameter of porcelain at bottom (cm)	40.0	30.0	30.0
Thickness of porcelain (cm)	2.5	2.5	2.5
Diameter of head part of bushing (cm)	45	30	50
Number and size of volts in each facility (mm)	8*M16	16*M12	24*M14
Type of support	Fixed	Fixed	Fixed

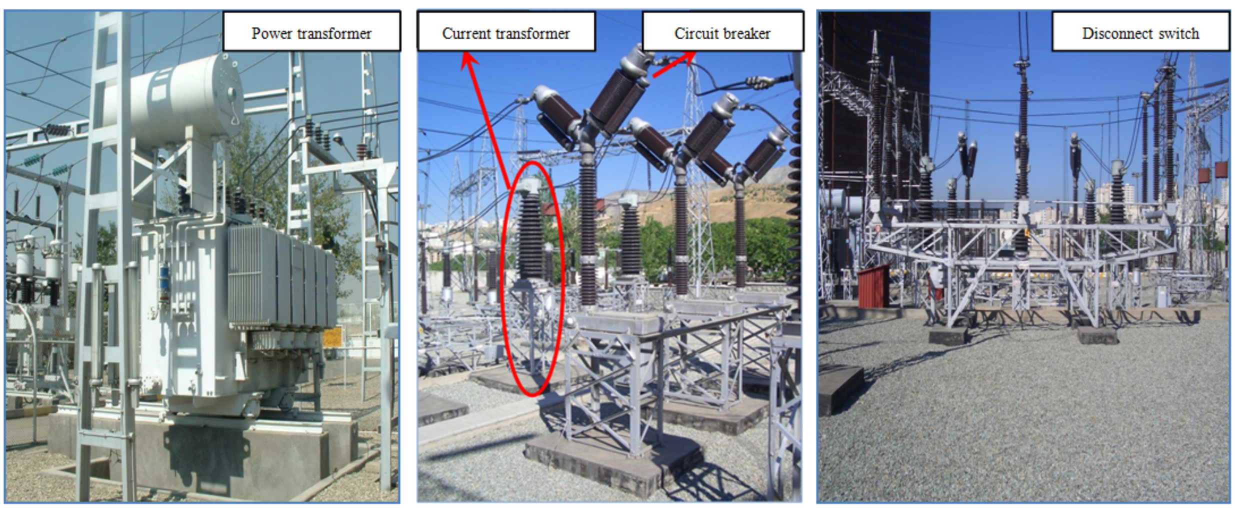

Fig. 4 Power transformer, current transformer, circuit breaker and disconnect switch at a substation in Tehran

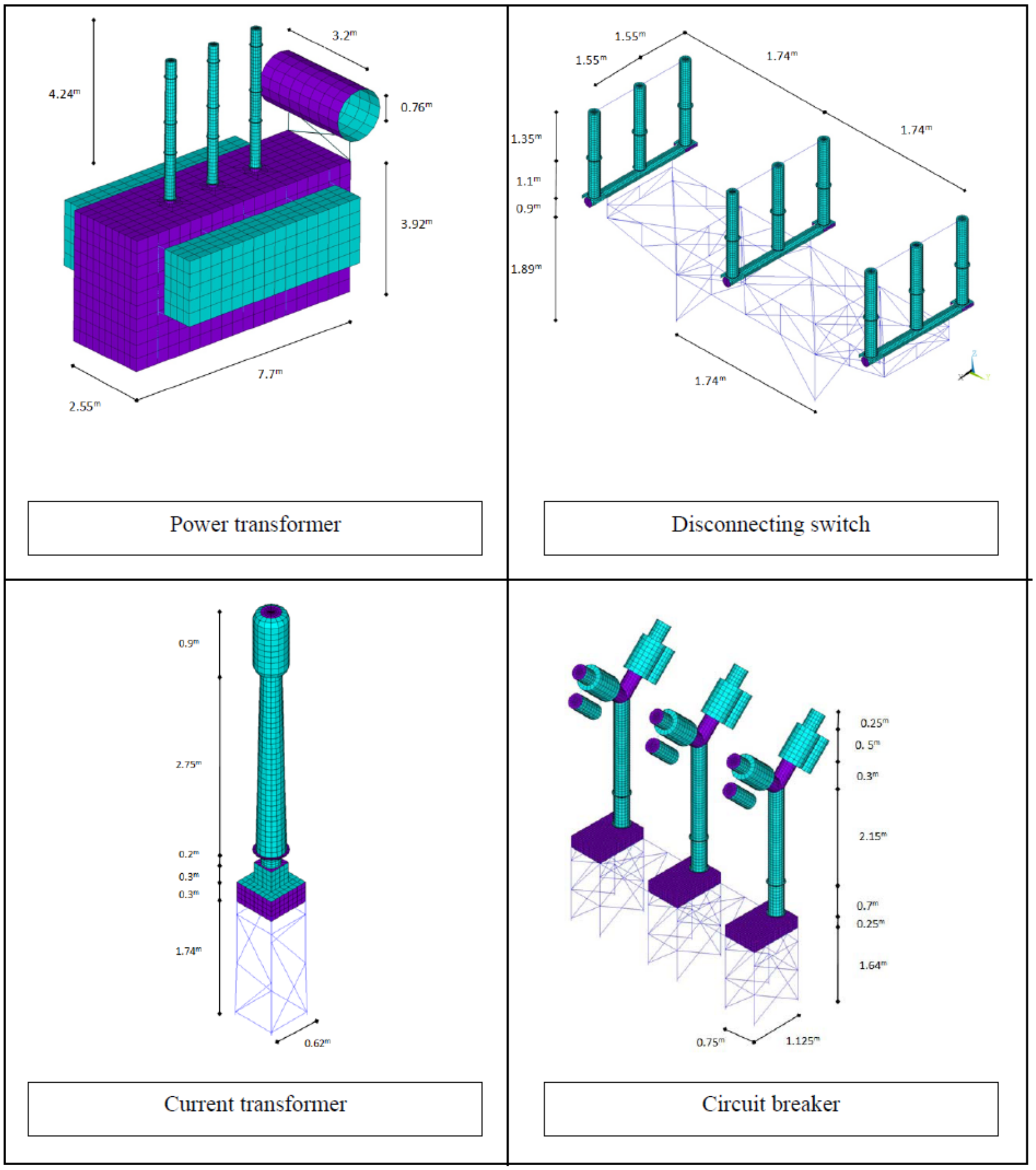

Fig. 5 Finite element models of power transformer, current transformer, circuit breaker and disconnect switch

3.1. Modal analysis

Modal analysis was performed to obtain the natural frequencies of the equipment. Table 3 shows the first 10 natural frequencies. In the results, first mode is frequency of the reservoir and not frequency of the bushing. Second mode is frequency of the bushings, which is affected by flexibility of the top plate of the main body. The bushings are mounted on top of the transformer's main body. In this regard, the most important factors that affect the natural frequencies are: stiffness of the main body, thickness and stiffeners of the top plate of the main tank (as support of the bushing). These factors are important on second to seventh modes. The eighth mode is torsion of the oil reservoir. The ninth and tenth modes are frequencies of the radiators influenced by stiffness of lateral plates of the main body.

Table 3 Natural frequency (HZ) of equipment by mode

	Mode									
	1	2	3	4	5	6	7	8	9	10
Power transformer	0.297	1.875	1.937	1.994	2.019	2.036	2.040	2.096	2.200	2.304
Current transformer	3.3757	3.3788	25.408	26.155	46.188	46.767	62.442	62.667	66.784	67.079
Disconnect switch	2.0903	2.0959	3.8913	4.7164	4.7874	4.6019	4.9707	2.1020	5.2123	5.2243
Circuit breaker	1.8428	1.8435	1.8463	1.8906	1.9022	1.9027	8.5152	8.5394	8.5428	8.8908

First natural frequencies of the four different types of the transformers obtained from experimental tests by Villaverde et al. [18] are 2.4 to 4.1 Hz. In our results, frequency of the first mode of the bushings is obtained 1.876 Hz. As result, the natural frequencies of the bushings are not fairly far from the measured values. There are some reasons to explain the differences between the Villaverde et al. and the obtained results as below:

1- The transformers are made by different manufacturers and their structural details such as thickness of plates, stiffeners, gaskets and so on are not the same.

2- The most important reason is that they did not consider the main body of the transformer. It has a very important effect on dynamic properties of the bushings, and considering the body of the transformer reduces the natural frequencies. To confirm that, Khalvati (2011) in an experimental study on low voltage equipments in IIEES showed considering the substructure (main body in the power transformer) decrease natural frequency of the equipments by three times [18].

3.2. Time history analysis

Time history analysis was done for the equipment using 50 recorded near or far-field ground motions (Tables 4 and 5). For example, Figures 6 and 7 show the maximum response spectrum of the power transformer on several levels for far and near-field strong motion, respectively, for the 1978 Tabas and 2004 Hasan Keyf records. The results reveal that the maximum responses occurred at the top of the equipment.

Table 4 Specifications of recorded motions in near field.

Record	Date	MB*	MS*	MN*	ML*	PGA (L)[1]	PGA (V)[2]	PGA (T)[3]	Soil type	L[4]
Bam	12/26/2003			6.3		0.799	0.989	0.636	2	14
Chalan Choolan	3/31/2006				6.2	0.432	0.524	0.357	2	6
Chatrood	2/22/2005			6.4		0.057	0.053	0.1	1	20
Deyhook	9/16/1978	6.4	7.4			0.331	0.179	0.411	1	10
Fin 1	3/25/2006				6	0.171	0.149	0.194	2	16
Gomishan	10/7/2004				6.2	0.092	0.029	0.087	3	20
Hasan Keyf	5/28/2004	6.2				0.922	0.415	0.501	3	16
Tabl	9/10/2008				6.1	0.089	0.07	0.085	1	19
Talesh	11/4/1978	6.2	6			0.28	0.139	0.213	2	14
Tomban	9/10/2008				6.1	0.597	0.314	0.571	1	15

*Magnitudes: MB: body wave; MS: surface wave; MN: Nuttli; ML: local
1 Longitudinal
2 Vertical
3 Transverse
4 Distance from earthquake center in km

Table 5 Specifications of recorded motions in far field.

Record	Date	MB*	MS*	MN*	ML*	PGA (L)[1]	PGA (V)[2]	PGA (T)[3]	Soil type	L[4]
Abbar	6/20/1990	6.4	7.7			0.635	0.546	0.546	2	41
Abaragh	12/26/2003			6.3		0.171	0.089	0.111	1	50
Abgarm	6/22/2002			6.2		0.12	0.051	0.13	3	24
Ahmadi 1	2/28/2006				6.1	0.119	0.054	0.139	2	43
Ahmadi 2	2/14/2003				6.1	0.072	0.016	0.066	2	40
Babol	5/28/2004	6.2				0.014	0.012	0.013	4	122
Bandar Khamir1	11/27/2005	6.2				0.016	0.009	0.018	2	30

Bandar Khamir2	9/10/2008				6.1	0.02	0.01	0.018	2	26
Darreh Asbar	3/31/2006				6.2	0.109	0.074	0.123	1	27
Davaran	2/22/2005			6.4		0.056	0.033	0.048	1	72
Dorood	3/31/2006				6.2	0.037	0.033	0.036	1	22
Fork	9/10/2008				6.1	0.011	0.008	0.009	2	172
Ghale Ganj	2/28/2006				6.1	0.012	0.006	0.011	2	126
Ghaleno Kharaqan	1/10/2005				6.1	0.029	0.011	0.037	2	72
Gorgan	1/10/2005				6.1	0.061	0.031	0.044	3	34
Hamedan5	3/31/2006				6.2	0.025	0.009	0.021	1	140
Hasan Langi	9/10/2008				6.1	0.03	0.008	0.022	3	119
Horjand	2/22/2005			6.4		0.047	0.068	0.041	1	31
Iincheh Borun	1/10/2005				6.1	0.163	0.031	0.078	3	40
Kaboodar Ahang	6/22/2002				6.2	0.087	0.071	0.166	2	58
Kooshk-e Olya	3/4/1999	6.2	6.5			0.049	0.042	0.036	1	63
Moalem Kelayeh	5/28/2004	6.2				0.297	0.079	0.272	2	76
Noor	5/28/2004	6.2				0.05	0.019	0.06	3	44
Noshahr	5/28/2004	6.2				0.073	0.038	0.107	4	33
Qaen	11/27/1979	6.1	7.1			0.217	0.114	0.142	1	52
Qahrvand	6/22/2002				6.2	0.052	0.023	0.085	2	91
Qeshm	6/28/2006				6.1	0.019	0.027	0.026	1	45
Ravar	2/22/2005			6.4		0.121	0.034	0.075	1	54
Razan	6/22/2002				6.2	0.184	0.135	0.201	3	33
Rezvan	3/25/2006				6	0.121	0.035	0.103	1	32
Shirinsu	6/22/2002				6.2	0.18	0.093	0.128	1	57
Shool Abad	3/31/2006				6.2	0.041	0.017	0.038	1	59
Sirik	9/10/2008				6.1	0.021	0.005	0.028	3	131
Suza	9/10/2008				6.1	0.168	0.113	0.165	1	25
Suza 2	11/27/2005	6.2				0.327	0.129	0.209	1	22
Tabas	9/16/1978	6.4	7.4			0.846	0.717	0.898	2	54
Taleghan	5/28/2004	6.2				0.096	0.063	0.121	2	77
Tomban 2	6/28/2006				6.1	0.518	0.442	0.308	1	28
Tooshk Absard	3/31/2006				6.2	0.328	0.237	0.394	1	38
Zarand	2/22/2005			6.4		0.323	0.309	0.241	3	31

*Magnitudes: MB: body wave; MS: surface wave; MN: Nuttli; ML: local
1 Longitudinal
2 Vertical
3 Transverse
4 Distance from earthquake center in km

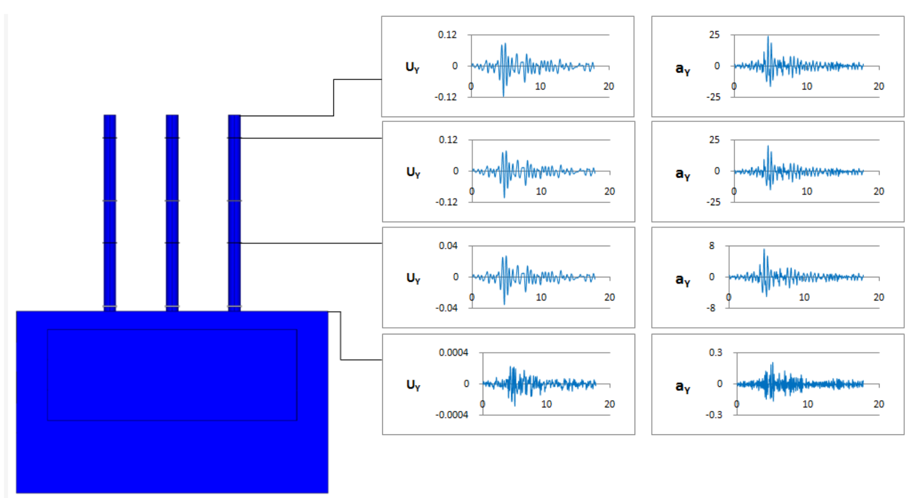

Fig. 6 Maximum response spectrum of power transformer under far-field strong motion (the 1978 Tabas record)

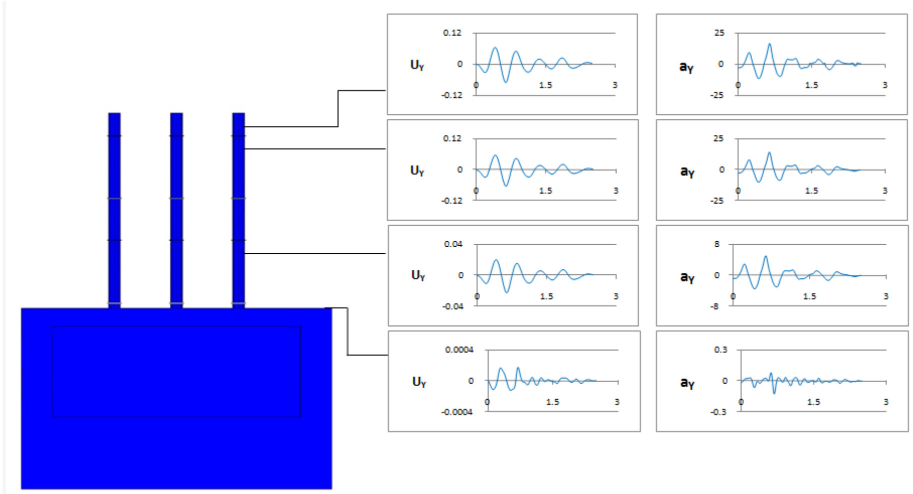

Fig. 7 Maximum response spectrum of power transformer under near-field strong motion (the 2004 Hasan Keyf).

3.3. Modeling verification

Villaverde et al. (2001) [9] performed experimental field tests and analytical studies to qualify ground motion amplification at the base of bushings mounted on electric substation transformers caused by the flexibility of the transformer tank and turrets to which they were connected. The study included field tests of typical transformers to obtain their natural frequencies and damping ratios, the development of simple analytical models that closely match the experimental data, and the calculation of the transformer dynamic response under earthquake excitation using analytical models. For each excitation, the peak transformer response and corresponding ground motion amplification factors were calculated at the base of the 500 kV and 230 kV bushings. These amplification factors were obtained by dividing the peak shear force at the base of the bushings by the corresponding shear force when the bushings were assumed to be mounted directly on the ground. They concluded that amplification factors for the 500 kV bushings are within the amplification factor of 2.0 specified by IEEE 693 (IEEE, 1997). However, the 230 kV bushings exceeded the IEEE 693 amplification factor (Villaverde et al., 2001) [9].

To verify the modeling in the present study, the transformer models are analyzed using records from the Northridge earthquake in 1999 recorded at the Olive View Hospital near-fault station (acceleration time histories from PEER). The amplification factors are calculated as described for Villaverde et al. (2001) [9]. In that study, the Pauwels and Westinghouse transformers are similar to the transformer used in the present study. Table 6 shows the comparison of the results. Since the type of transformer, dimensions and material specifications of the model are different from those in the previous research; the shear force differs from the results obtained from the present study. As indicated in Table 6, the amplification factor is more comprehensive than the one recommended by IEEE 693 (IEEE, 1997), JEAG-5003-1999 (JEA, 1999) or in the literature (e.g., Villaverde et al., 2001) [9].

Table 6 Comparison of amplification factors of modeled 230 kv power transformer and Westinghouse transformer [9]

Transformer	Transverse			Longitudinal		
	Shear force (N)		Amplification factor	Shear force (N)		Amplification factor
	ground	tank		ground	tank	
230 kv bushing of Westinghouse transformer	1274.9	3106.1	2.44	2056.3	5609.7	2.73
230 kv bushing of modeled transformer	1805.0	4992.4	2.77	2113.9	5725.9	2.71

We found experimental study by Gilani et al. [7] on response time histories of bushings, in those just records of an earthquake are considered. The tests are done just for bushing and they did not consider main body of the transformer due to weight and size limitation of the shaking table. Purpose of this test was the evaluation of IEEE 693-1997 requirements. In this report they concluded: “Field reconnaissance and observations from past earthquakes suggest that failures (oil leakage and slip of porcelain units) of similar bushings occurred at levels of ground shaking significantly lower than those to which the two bushings were subjected. The reason for this discrepancy in performance is somewhat unclear. However, it is likely that the IEEE procedures do not adequately capture the critical loading environment for bushings because the electrical equipment attached at the top of the bushing in the field are not included in the qualification and fragility testing.” Therefore, we did not find an experimental study on whole system of the transformer to verify the models by response time histories. We did verification by amplification factors of the bushings because in both of the following experimental studies, they measured and discussed on. In addition, IEEE 693 (1997 and 2005) obligates to consider the amplification factors in seismic design of the bushings as the most important factor in seismic design of this equipment.

4. Input Waves

JEAG-5003-1999 for power substation equipment recommends sine waves as input waves for the time history analysis based on 615 ground motion records of earthquakes in Japan (JEA, 1999) [4]. This technique is used to obtain seismic loads for the dynamic analysis of performance-based seismic design of insulators and bushings in the Seismic Design Guideline of Electric Systems in Iran. Since the most damaging dynamic behavior of structures occurs as a result of resonance, series containing one, two or three sine waves are created for each piece of equipment. The frequency of the sine waves is equal to the natural frequency of each piece of equipment, and amplitude *A* of the waves is equal to 0.1 g, 0.15 g, 0.2 g, 0.25 g, 0.3 g, 0.35 g, 0.4 g, 0.45 g and 0.5 g. Restricting the movement of equipment at the top of the bushing is important and requires interaction with adjacent equipment, and the acceleration response is necessary for the seismic design of the equipment. The maximum lateral translation and acceleration at the top of the equipment for 50 ground motion records and sinusoidal waves are compared to obtain the appropriate input sine waves.

The records are categorized into near-field or far-field ground motions (Tables 4-5). First, the displacement and acceleration of near-field records are compared with sine waves and the results of far-field records. Then, the wave that covers the median plus one standard deviation (84.1%) of displacement and acceleration response in the near field (most critical state) is evaluated and the results are summarized in Tables 7 and 8, except for the single sine wave. The results for full coverage of acceleration and displacement response and sine waves for the top of the power transformer are shown in Tables 9 and 10, respectively. If we compare the results of the equipments displacement and acceleration responses in Tables 7 and 8 (or Tables 9 and 10), it is clear that unlike the usual procedure where maximum acceleration is the criteria for seismic design, i.e. IEEE Standards 693-2005, these results indicate more critical states for displacement responses (e.g., current transformer or circuit breaker). In this case, the equipment designed based on maximum acceleration was damaged by exceeding the allowable displacement at the top of the bushings. Since the equipments in power substations are connected via conductors, this is highly significant and can easily damage the connected equipments.

Table 7 Evaluation of 84.1% coverage of displacement response by sine waves.

Amplitude	Current transformer		Power transformer		Circuit breaker		Disconnect switch	
	2 wave	3 wave	2 wave	3 wave	2 wave	3wave	2 wave	3 wave
0.1 g	no	no	no	no	no	no	no	no
0.15 g	no	no	no	no	no	no	no	no
0.2 g	no	no	no	no	yes	yes	no	no
0.25 g	no	no	no	yes	yes	yes	yes	yes
0.3 g	no	yes	no	yes	yes	yes	yes	yes
0.35 g	yes	yes	no	yes	yes	yes	yes	yes
0.4 g	yes	yes	yes	yes	yes	yes	yes	yes
0.45 g	yes	yes	yes	yes	yes	yes	yes	yes
0.5 g	yes	yes	yes	yes	yes	yes	yes	yes

Table 8 Evaluation of 84.1% coverage of acceleration response by sine waves

Amplitude	Current transformer		Power transformer		Circuit breaker		Disconnect switch	
	2 wave	3 wave	2 wave	3 wave	2 wave	3 wave	2 wave	3 wave
0.1 g	no	no	no	no	no	no	no	no
0.15 g	no	no	no	no	no	no	no	no
0.2 g	no	no	no	no	no	no	no	no
0.25 g	no	yes	no	yes	yes	yes	yes	yes
0.3 g	yes	yes	no	yes	yes	yes	yes	yes
0.35 g	yes	yes	no	yes	yes	yes	yes	yes
0.4 g	yes	yes	yes	yes	yes	yes	yes	yes
0.45 g	yes	yes	yes	yes	yes	yes	yes	yes
0.5 g	yes	yes	yes	yes	yes	yes	yes	yes

Table 9 Evaluation of full coverage of displacement response by sine waves

Amplitude	Current transformer		Power transformer		Circuit breaker		Disconnect switch	
	2 wave	3 wave	2 wave	3 wave	2 wave	3 wave	2 wave	3 wave
0.1 g	no	no	no	no	no	no	no	no
0.15 g	no	no	no	no	no	no	no	no
0.2 g	no	no	no	no	no	no	no	no
0.25 g	no	no	no	no	no	no	no	no
0.3 g	no	no	no	no	no	no	no	no
0.35 g	no	no	no	yes	no	no	no	no
0.4 g	yes	yes	yes	yes	yes	yes	yes	yes
0.45 g	yes	yes	yes	yes	yes	yes	yes	yes
0.5 g	yes	yes	yes	yes	yes	yes	yes	yes

Table 10 Evaluation of full coverage of acceleration response by sine waves

Amplitude	Current transformer		Power transformer		Circuit breaker		Disconnect switch	
	2 wave	3 wave	2 wave	3 wave	2 wave	3 wave	2 wave	3 wave
0.1 g	no	no	no	no	no	no	no	no
0.15 g	no	no	no	no	no	no	no	no
0.2 g	no	no	no	no	no	no	no	no
0.25 g	no	no	no	no	no	no	no	no
0.3 g	no	no	no	no	no	no	no	no
0.35 g	yes	yes	no	yes	no	no	no	no
0.4 g	yes	yes	yes	yes	yes	yes	yes	yes
0.45 g	yes	yes	yes	yes	yes	yes	yes	yes
0.5 g	yes	yes	yes	yes	yes	yes	yes	yes

4.1. Power transformer

Figure 8 shows the displacement results in near-field records, where three sine waves with amplitude of 0.25 g cover the total results. Figure 9 shows the acceleration results in the near-field records where three sine waves with amplitude of 0.3 g cover the total results. In the far field, the results are less than 0.04 m, thus three sine waves with amplitude of 0.2 g are adequate (Figure 10). For acceleration, three sine waves with amplitude of 0.2 g cover the total records except in the case of the 1978 Tabas earthquake (Figure 11).

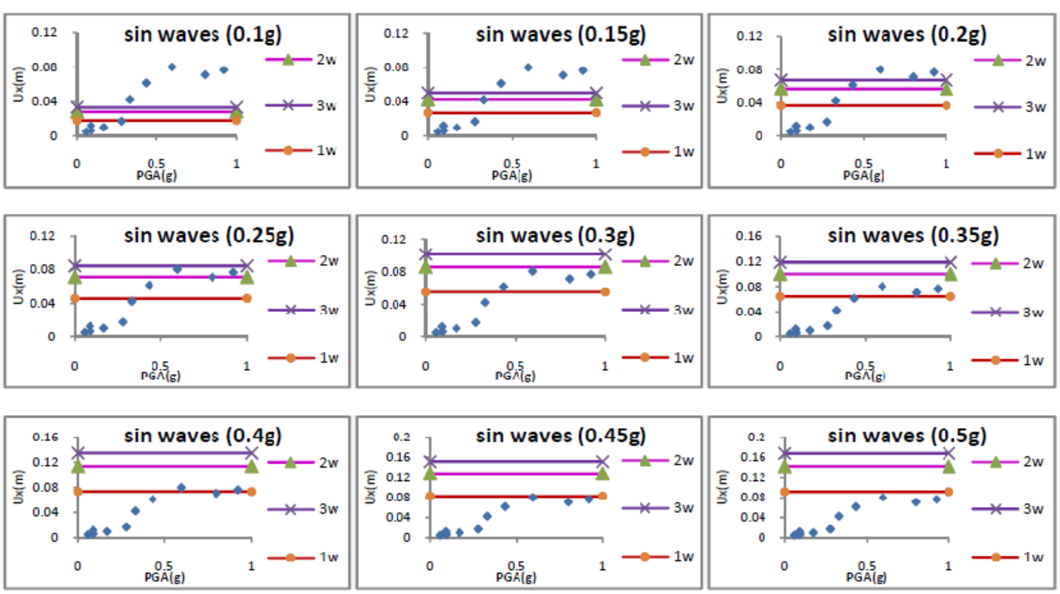

Fig. 8 Comparison of displacement results for top of power transformer bushing under near-field ground motion and sine waves

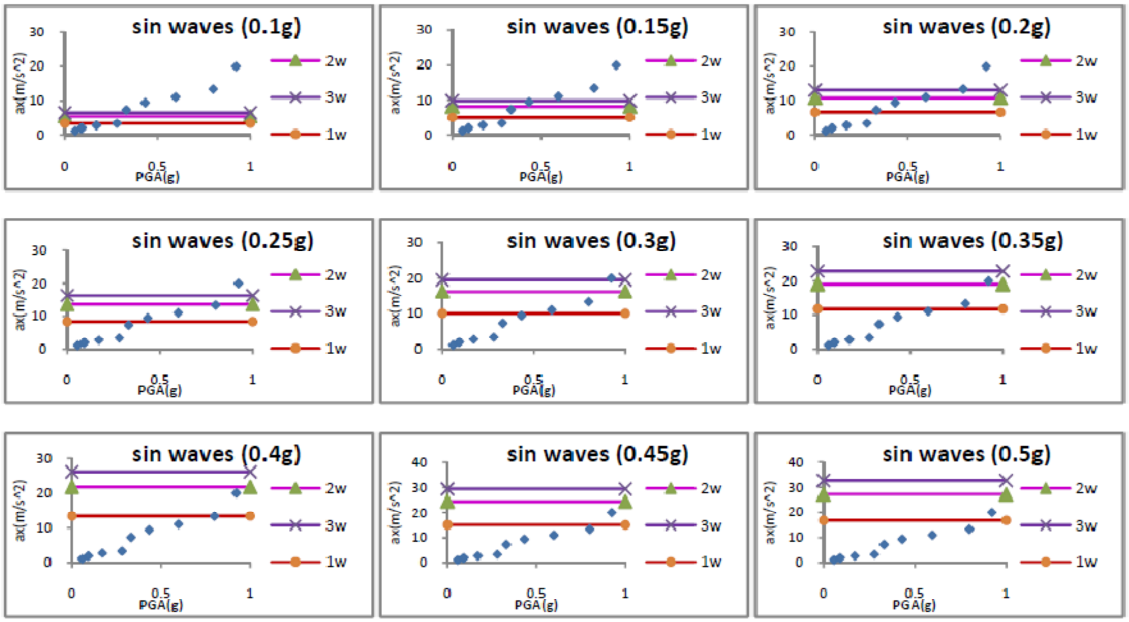

Fig. 9 Comparison of acceleration results for top of power transformer bushing under near-field ground motion and sine waves

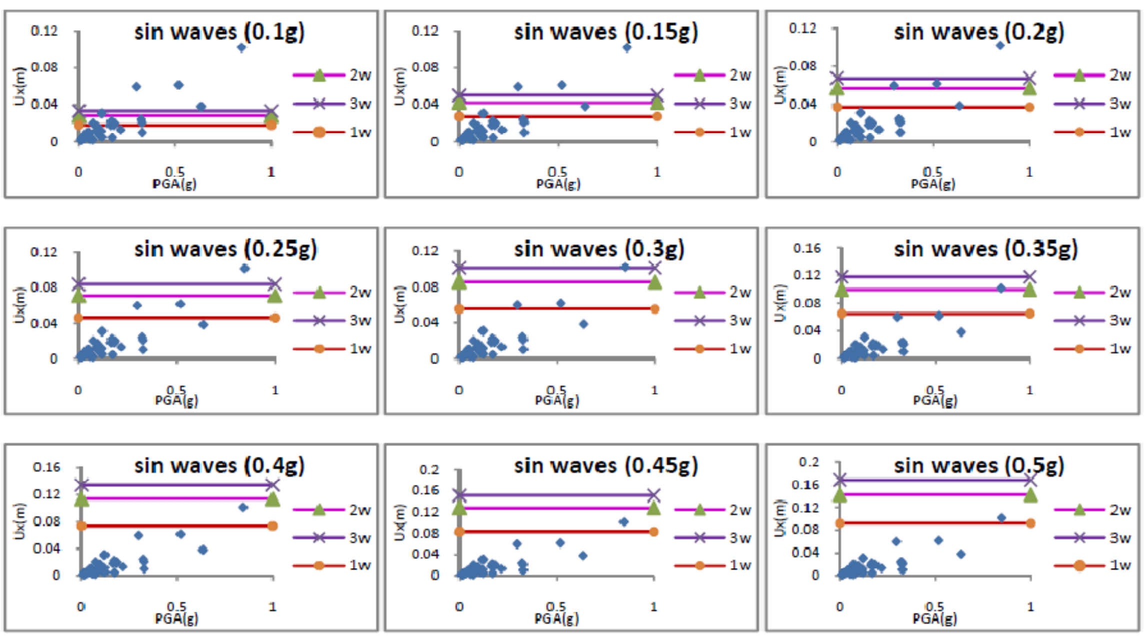

Fig. 10 Comparison of displacement results for top of power transformer bushing under far-field ground motion and sine waves

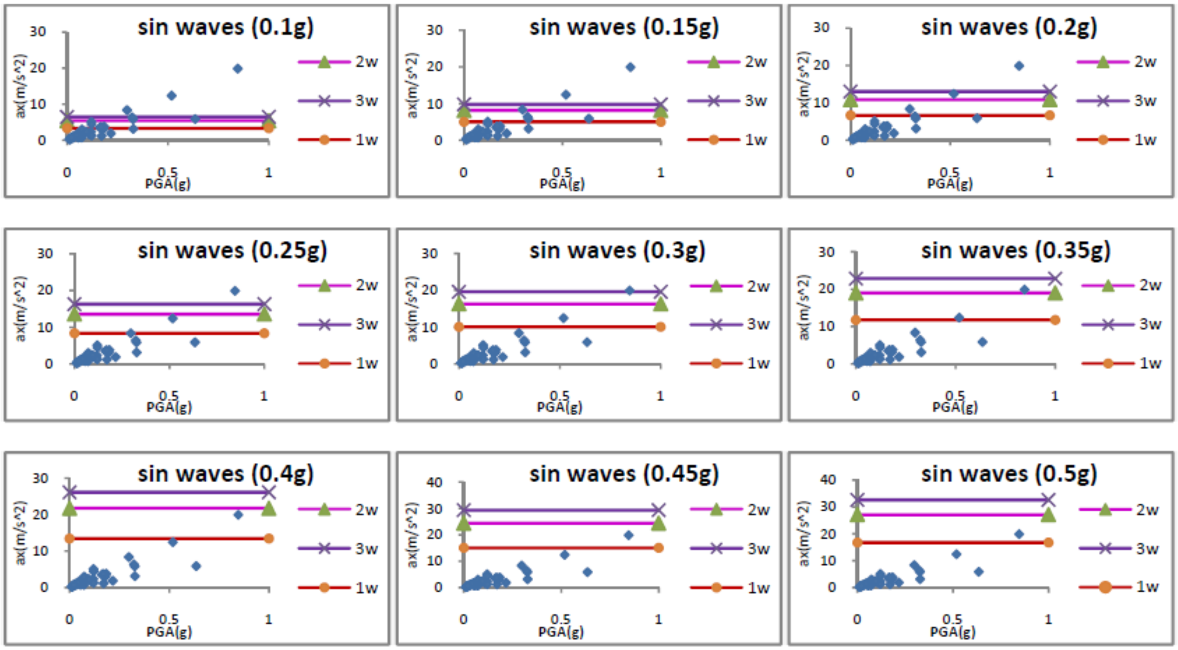

Fig. 11 Comparison of acceleration results for top of power transformer bushing under far-field ground motion and sine waves

4.2. Current transformer

Figure 12 shows the comparison of displacement results for the current transformer in the near field where three sine waves nearly cover the results with a domain of 0.35 g. Figure 13 shows the acceleration results with adequate coverage by three sine waves with an amplitude of 0.3 g. For the far field, Figure 14 shows the displacement results with adequate coverage with three waves with amplitude of 0.3 g and Figure 15 shows the acceleration results for nearly complete coverage with three sine waves and amplitude of 0.25 g.

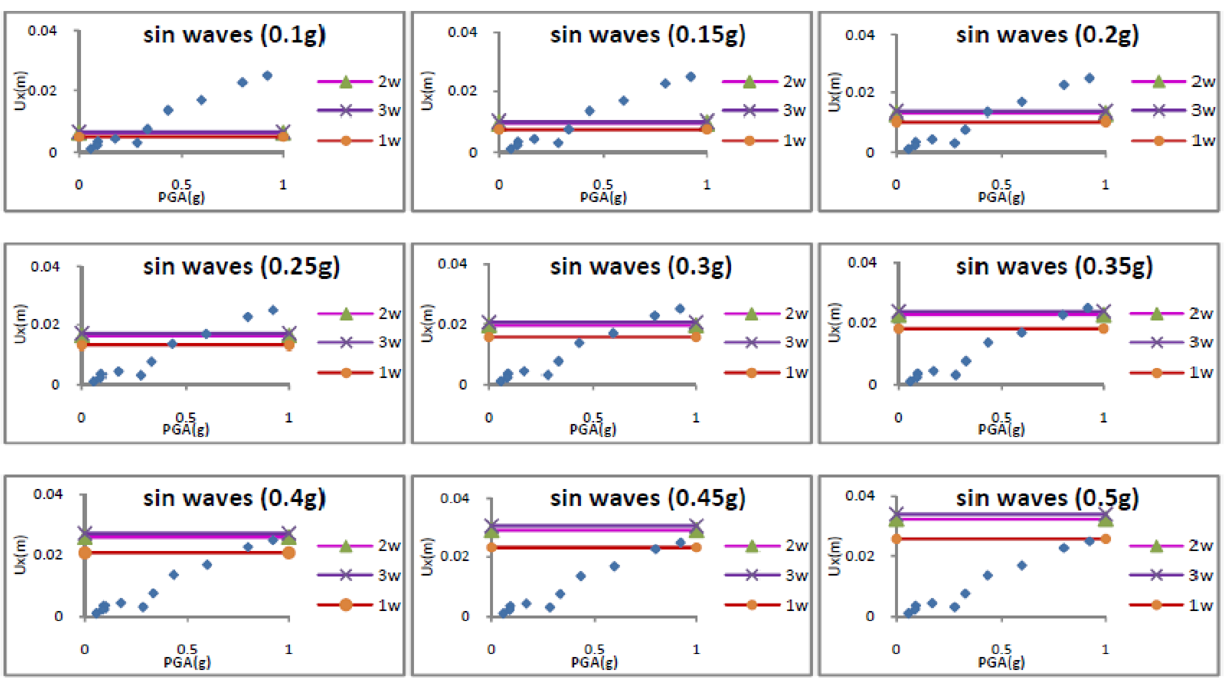

Fig. 12 Comparison of displacement results for top of current transformer bushing under near-field ground motion and sine waves

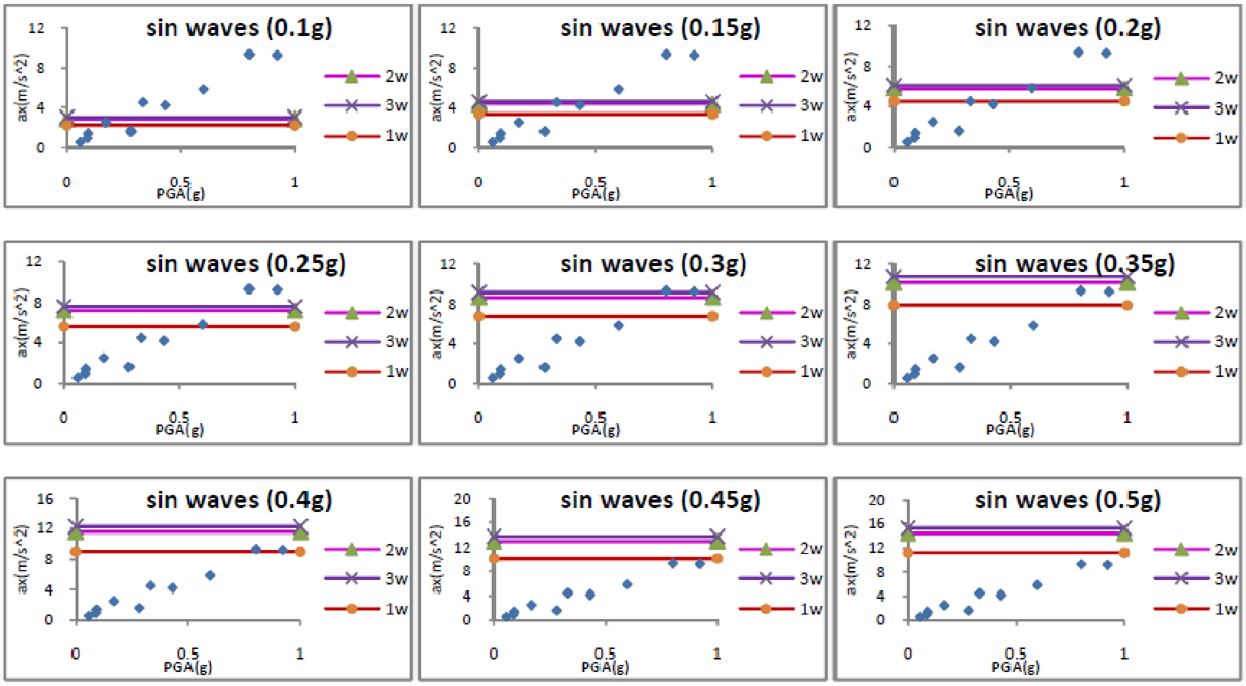

Fig. 13 Comparison of acceleration results for top of current transformer bushing under near-field ground motion and sine waves

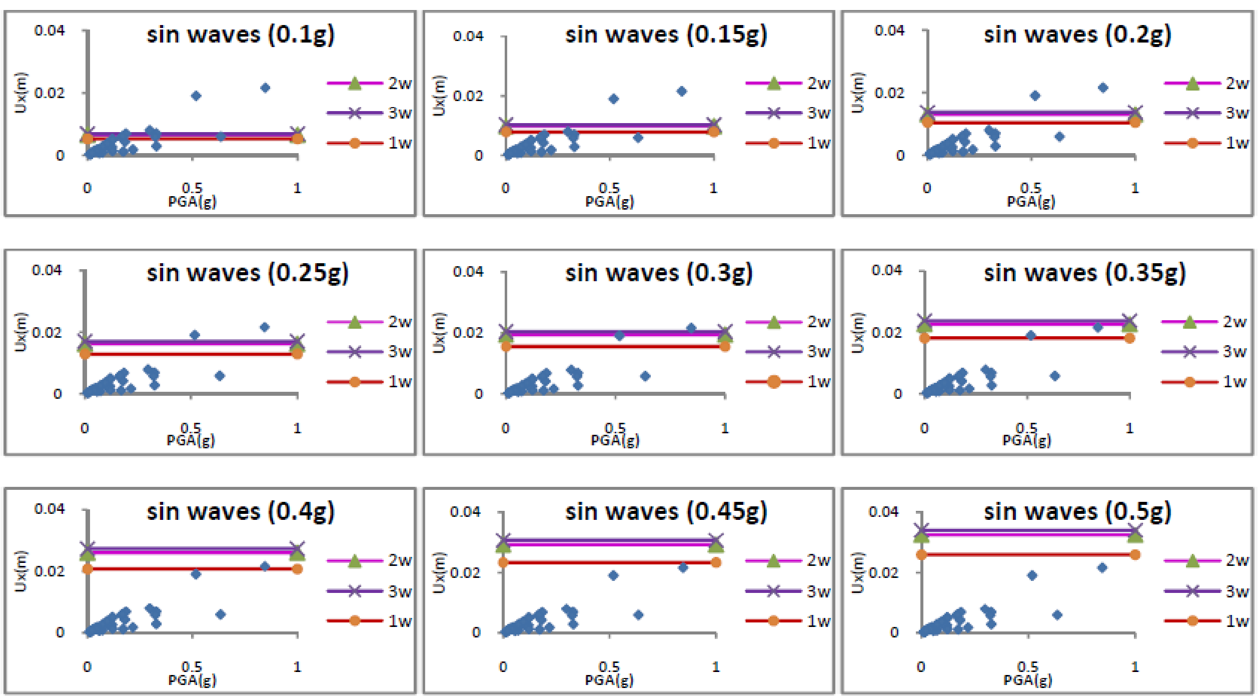

Fig. 14 Comparison of displacement results for top of current transformer bushing under far-field ground motion and sine waves

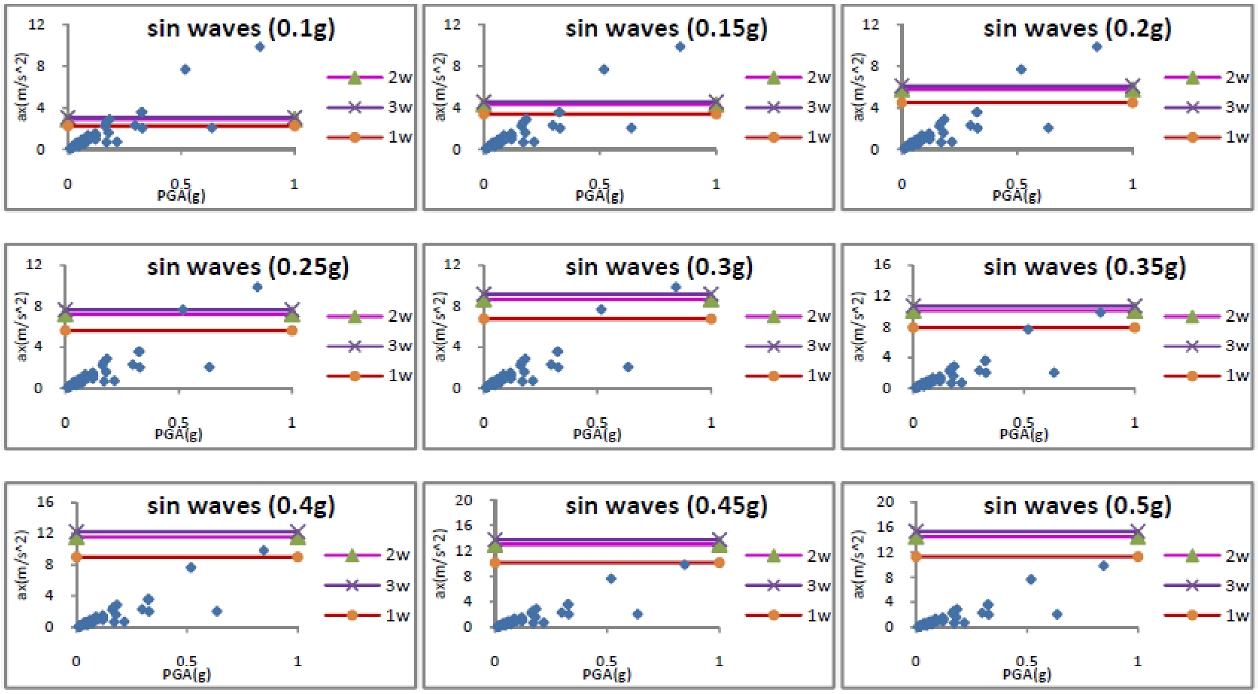

Fig. 15 Comparison of acceleration results for top of current transformer bushing under far-field ground motion and sine waves

4.3. Disconnect switch

Figure 16 shows the displacement results (excluding the 1978 Tabas record) in the near field for three sine waves with an amplitude of 0.25 g. Figure 17 shows the acceleration results for two sine waves adequate coverage with an amplitude of 0.35 g. Figure 18 shows, in the far field, the displacement results for two sine waves with an amplitude of 0.15 g as a result of aggregation in the lower range. Figure 19 shows the acceleration results where two or three sine waves are nearly covered with amplitude of 0.15 g.

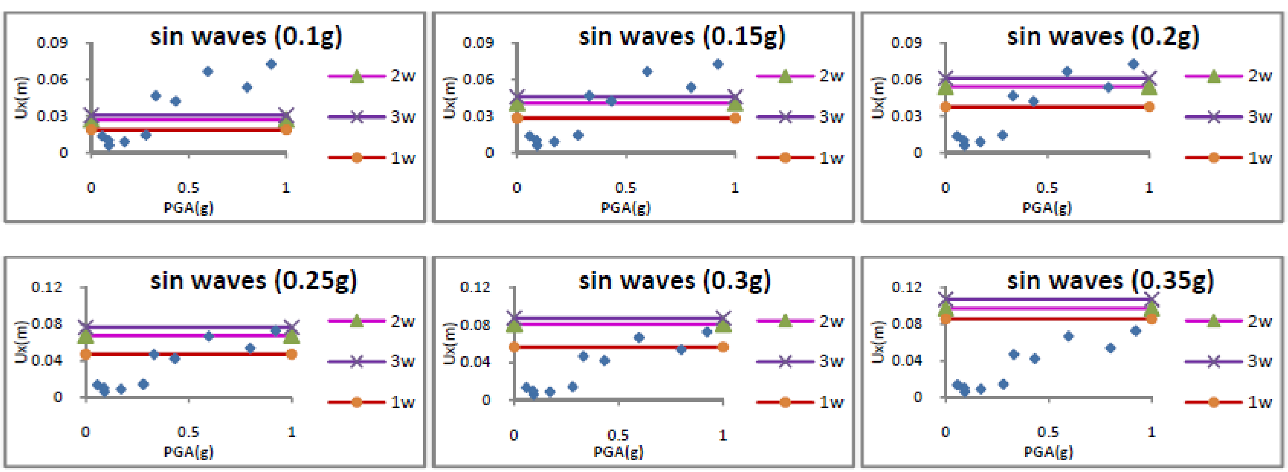

Fig. 16 Comparison of displacement results for top of disconnect switch bushing under near-field ground motion and sine waves

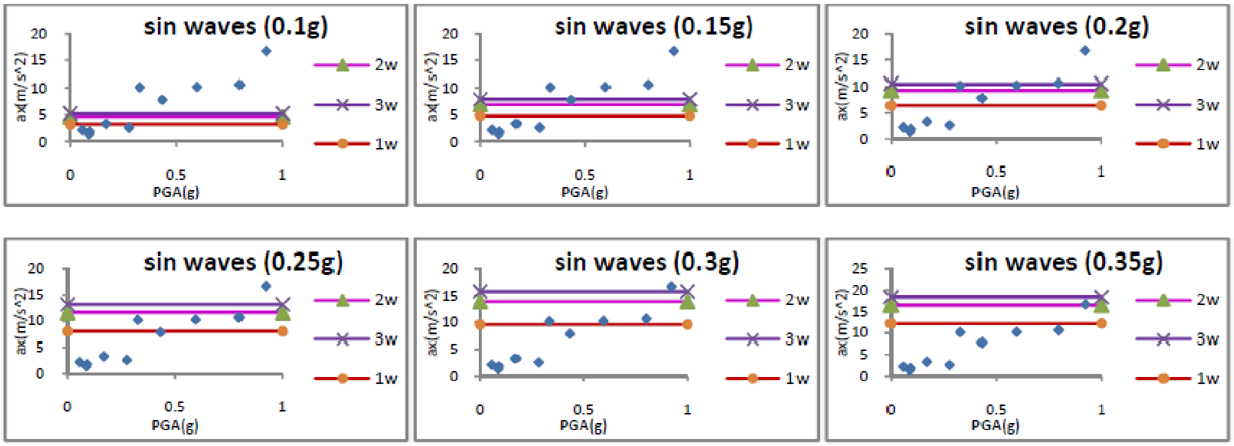

Fig. 17 Comparison of acceleration results for top of disconnect switch bushing under near-field ground motion and sine waves

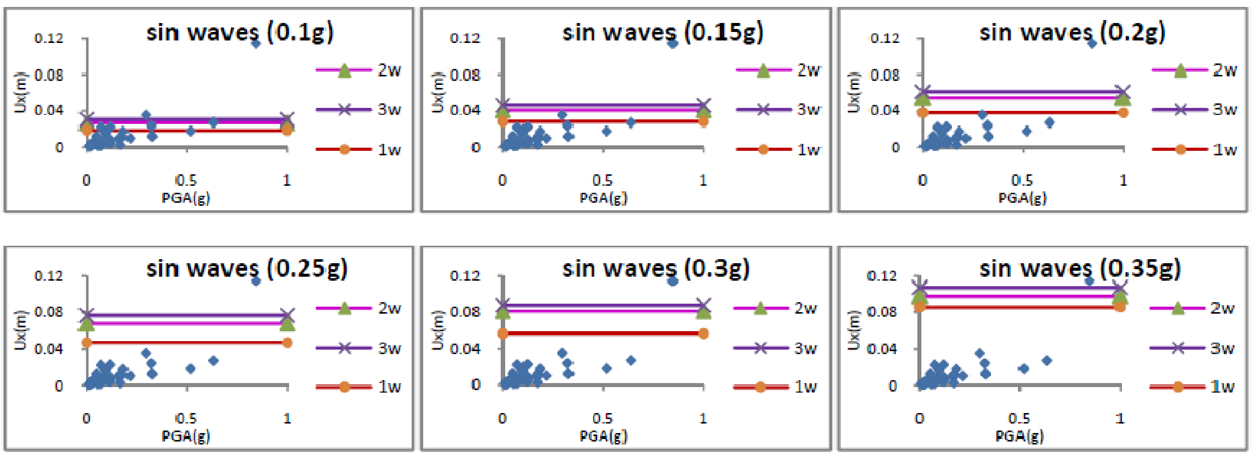

Fig. 18 Comparison of displacement results for top of disconnect switch bushing under far-field ground motion and sine waves

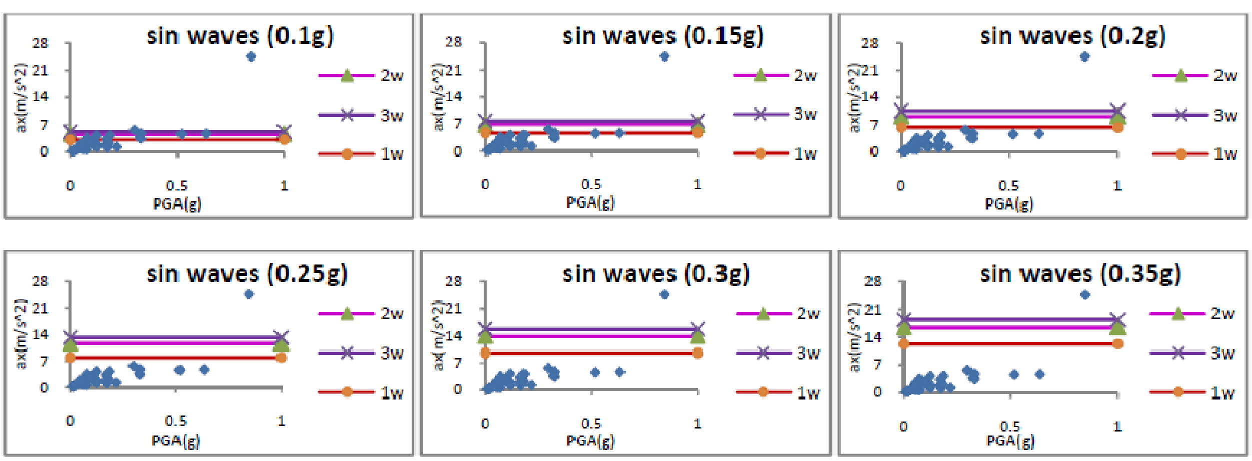

Fig. 19 Comparison of acceleration results for top of disconnect switch bushing under far-field ground motion and sine waves

4.4. Circuit breaker

As seen in Figures 20 and 21, in the near field, the displacement and acceleration results show three sine waves with amplitude of 0.25 g cover the results. In the far field, Figures 22 and 23 show displacement and acceleration results where three sine waves with amplitude of 0.15 g adequately cover the results.

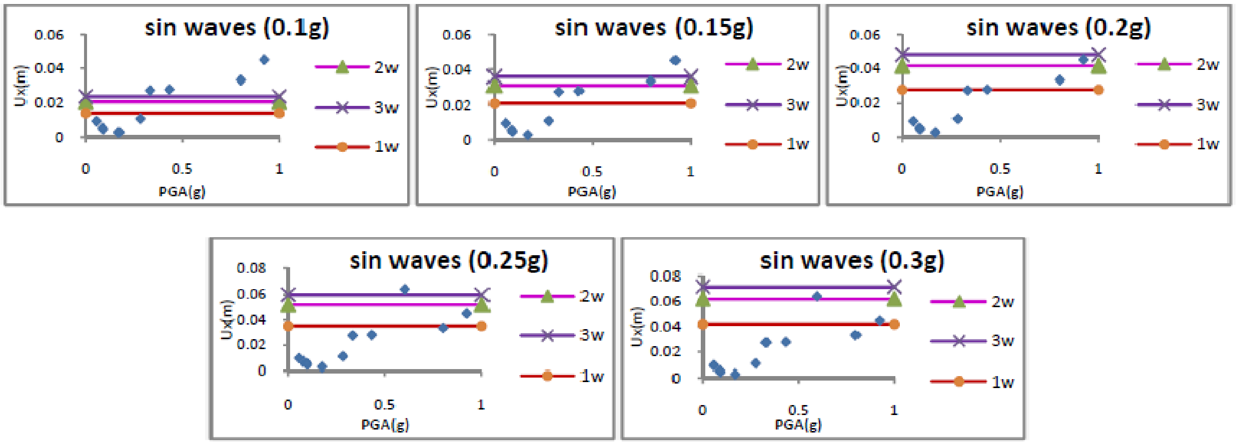

Fig. 20 Comparison of displacement results for top of circuit breaker bushing under near-field ground motion and sine waves

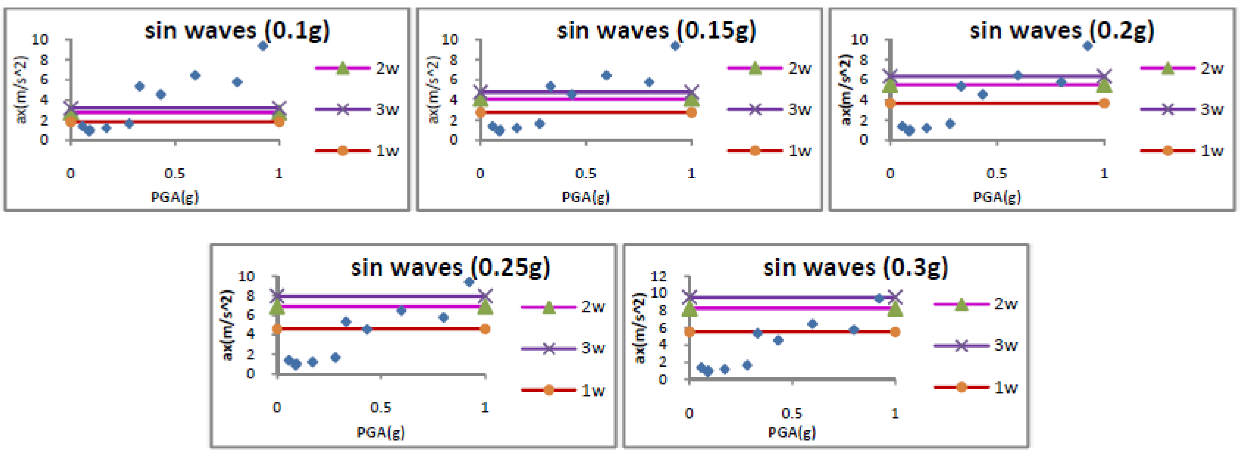

Fig. 21 Comparison of acceleration results for top of circuit breaker bushing under near-field ground motion and sine waves

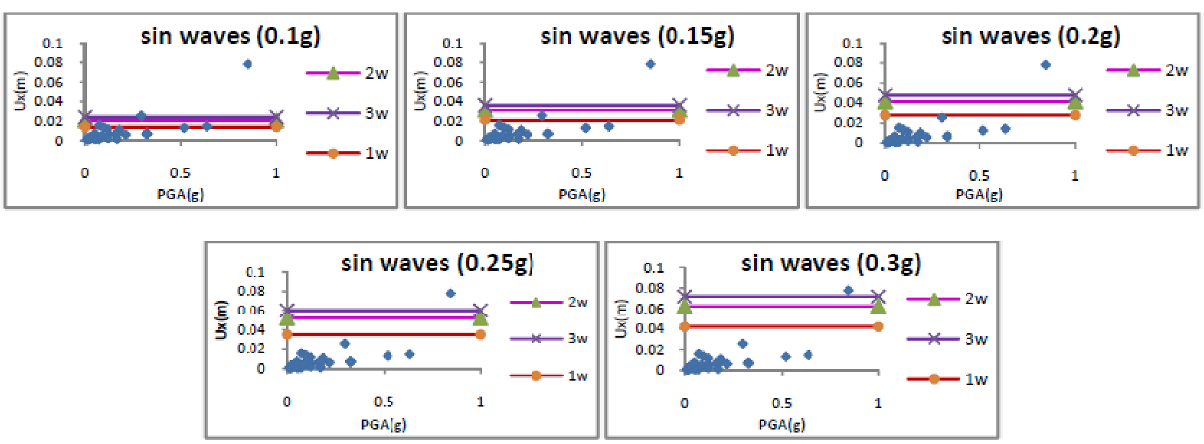

Fig. 22 Comparison of displacement results for top of circuit breaker bushing under far-field ground motion and sine waves

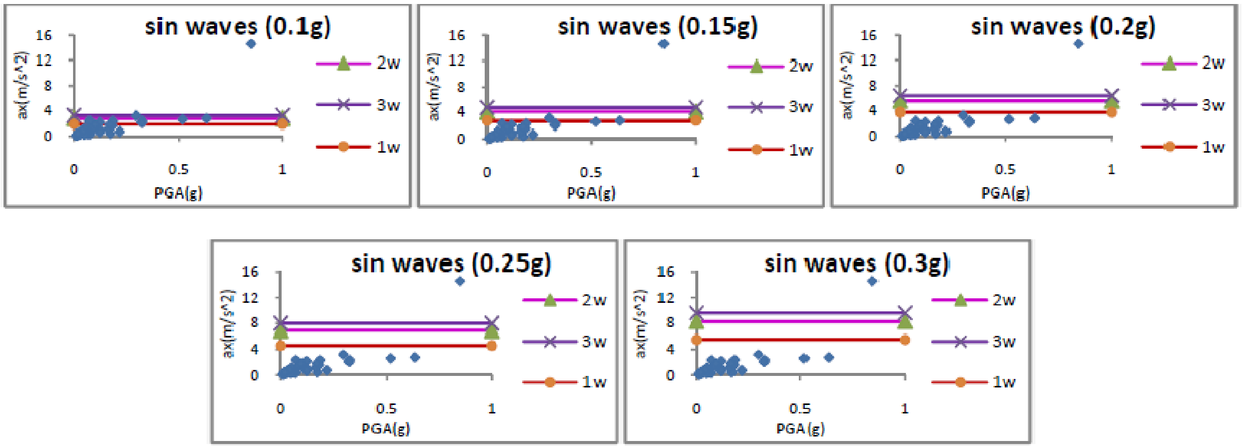

Fig. 23 Comparison of acceleration results for top of circuit breaker bushing under far-field ground motion and sine waves

5. Response for Near Field and Far Field

The average responses of the equipment were compared for near and far-field ground motions (Table 11). The ratio of acceleration response of near-field to far-field records are 2.45, 2.75, 2.78 and 2.66 for the power transformer, current transformer, live-tank circuit breaker and disconnect switch, respectively, with a mean value of 2.66. The ratio of displacement response for the near-field to far-field records are 2.38, 2.85, 2.83 and 2.84 for the power transformer, current transformer, live-tank circuit breaker and disconnecting switch, respectively, with a mean value of 2.73. As can be seen, the lowest value for both field results is for the power transformer. In general, the results for the near field are at least twice as high as the results for the far field (Table 11). These records can be employed to obtain the proposed suitable input wave.

6. Discussion and Conclusion

1) This research proposed a method to derive input waves for dynamic analysis of the power substation equipments in place of original records from seismic events in Iran. The technique recommended by the Japanese Guidelines employs a single degree-of-freedom model composed of a lumped mass and spring, while in this study, the equipments are modeled in detail using 3-D FEM to verify the technique for Iran. The results for 50 field records and the sine waves are compared for the far and near fields to propose the final appropriate sinusoidal wave for the equipments in Iran.

2) Unlike the usual procedure where maximum acceleration is the criteria for seismic design, these results indicate more critical states for displacement responses (e.g., current transformer). Since the equipments in power substations are connected via conductors, this is highly significant and can easily damage to the connected equipments.

3) Results for the near field were at least twice as high as the results in the far field (Table 11). These records can be employed to obtain a suitable input wave. The ratio of acceleration response in the near field to far field for the power transformer, current transformer, live-tank circuit breaker and disconnect switch were 2.45, 2.75, 2.66 and 2.78, respectively. The ratio for the displacement response for the near field to far field was 2.38, 2.85, 2.84 and 2.83, respectively. The lowest value in both cases was for the power transformer. The mean values for the current transformer, live-tank circuit breaker and disconnect switch was 2.84 for displacement and 2.73 for acceleration.

4) The proposed input wave based on 84.1% coverage of responses for seismic analysis and design of the power transformer is two sine waves with amplitude of 0.4 g or three sine waves with amplitude of 0.25 g. For the current transformer, it is three sine waves with amplitude of 0.3 g or two sine waves with amplitude of 0.35 g. For the circuit breaker and disconnect switch, it is two or three sine waves with an amplitude of 0.25 g.

5) The proposed input wave based on full coverage of the responses for seismic analysis and design of the power transformer is two sine waves with amplitude of 0.4 g or three sine waves with amplitude of 0.35 g. For the current transformer, circuit breaker and disconnect switch, there are two or three sine waves with an amplitude of 0.4 g. Note that the recommended input wave in the Japan Guidelines for a power transformer is three sine waves with an amplitude of 0.5 g and, for the other equipment, is three sine waves with an amplitude of 0.3 g.

References

[1] Schiff A.J. Guide to improve earthquake performance of electric power systems, American Society of Civil Engineers, ASCE, 1999, 341 p.

[2] BHRC (Building and Housing Research Center), 2011, Iran Strong Motion Network (ISMN), Tehran, Iran.

[3] Sharif V. Near-field earthquake effects on the dynamic behavior of structures, Seminar Report, International Institute of Earthquake Engineering and Seismology, Tehran, Iran (in Farsi), 2002.

[4] Japan Electric Association (JEA). Earthquake Resistant Design Guideline for Electric Facilities in Power Substation, JEAG 5003-1999, Japan (in Japanese), 1999.

[5] Bellorini S, Bettinali F, Salvetti M, Zafferani G. Seismic

qualification of transformer high voltage bushings, IEEE Transaction on Power Delivery, 1998, No. 4, Vol. 13, pp. 1208-1213.
[6] Gilani A, Whittaker A, Fenves G.L, Fujlsaki E.M. Seismic Evaluation of 550 kV Porcelain Transformer Bushings, PEER Report 1999/05, Pacific Earthquake Engineering Research Center, University of California, Berkeley, 1999, 79 p.
[7] Gilani A, Whittaker A, Fenves G.L, Fujlsaki E.M. Seismic evaluation of 230 kV porcelain transformer bushings, Earthquake Spectra, 2001, Vol. 17, pp. 597-616. doi:http://dx.doi.org/10.1193/1.1427316.
[8] Kiureghian A.D, Sachman J, Hong K.J. Interaction in Interconnected Electrical Substation Equipment Subjected to Earthquake Ground Motions, PEER Report 1999/01, Pacific Earthquake Engineering Research Center, University of California, Berkeley, 1999.
[9] Villaverde R, Pardon C.G, Carnalla S. Ground motion amplification at flange level of bushings mounted on electric substation transformers, Earthquake Engineering and Structural Dynamics, 2001, Vol. 30, pp. 621-632.
[10] Recommended Practices for Seismic Design of Substations, IEEE Standards 693-2005, IEEE, USA. doi: 10.1109/IEEESTD.2006.246239, 2006.
[11] Matt H, Filiatrault A. Seismic Qualification Requirements for Transformer Bushings, PEER Report SSRP- 2003/12, Pacific Earthquake Engineering Research Center, University of California, Berkeley, 2004, 9 p.
[12] Su F, Zeng Y, Anderson J.G. Input Motions for Earthquake Simulator Testing of Electric Substation Equipment (408), final project report, Seismological Laboratory/174, University of Nevada, Reno, Nevada, 2004, 61 p.
[13] Takhirov S.M, Fenves G.L, Fujisaki E, Clyde D. Ground Motions for Earthquake Simulator Qualification of Electrical Substation Equipment, PEER-2004/07, Pacific Earthquake Engineering Research Center, University of California, Berkeley, 2004, 183 p.
[14] Saadeghvaziri M.A, Feizi B, Kempner L, Alston D. On seismic response of substation equipment and application of base isolation to transformers, IEEE Transactions on Power Delivery, 2010, No. 1, Vol. 25, pp. 177-186.
[15] Koller M.G, Hässig M, Thomassin S. Natural frequencies of power transformers and their consequence, Proceedings of the 14th European Conference on earthquake Engineering, 30 August-3 September, Ohrid, Macedonia, 2010, Vol. 7, pp. 5188-5193.
[16] Bastami M. Seismic Reliability of Power Supply System Based on Probabilistic Approach, PhD thesis, Kobe University, Japan, 2007.
[17] Khalvati A.H, Hosseini M, Mohammadpour S. Seismic behavior of 63 kV and 132 kV substation post insulators with flexible conductors: an experimental approach, Journal of Seismology and Earthquake Engineering, No. 2, Vol. 13. pp. 72-99.
[18] Villaverde R, Pardon C.G, Carnalla S. Ground motion amplification at base of bushings mounted on electric substation transformers, A Technical Report of Research Supported by PEER/PG&E, Under Award No. PGE-09566, 2001.
[19] Khalvati A.H. Experimental and analytical evaluation of low voltage post insulators used to propose relevant seismic fragility functions, IIEES, PhD Thesis, Tehran, Iran, 2011.